

# **Multiple Focus Ultrasound Transducer With Lens for High Intensity Thermal Therapy**

Ashraf Talaat Ibrahim

Elec.,Eng.,Dept., Faculty of engineering, Alexandria University, Alexandria Egypt.

[ashraftalaat@yahoo.com](mailto:ashraftalaat@yahoo.com)

## **Abstract**

The diameters of thermal lesions generated by single-focus transducers are on the order of a few millimeters, which are usually small compared to the diameter of the tumors volume. The combination of a single transducer and an acoustic lens incorporating a 2-D grid of "elements" can produce multiple foci. Thermal lesion volumes generated by these multi-focus lens/transducer combinations [LTC] may be greater than those generated by single-focus spherical transducers. Compared to phased array designs, which can also generate multi-focus fields, LTCs are simple, inexpensive, and may offer greater flexibility for producing complex focus patterns, due to the greater number of elements. However, unlike phased arrays, whose elements can produce amplitude as well as phase modulation, LTCs can only use phase modulation because all LTC elements are activated by a single source. A theoretical evaluation of the ability of LTC designs to generate large thermal lesions for high temperature thermal treatments is presented. A design method, based on the pseudoinverse method, was developed to determine uniform amplitude activation signals required for LTCs to generate specified multi-focus fields. We demonstrate that LTC "phase only modulation" has very small effects on thermal lesion shape and size. To use LTCs for thermal lesion formation, longer exposure durations of 50s are suggested even though variable blood flow may produce large thermal dose changes in the field. The effect of focus spacing and number of foci produced by the LTC on the shape and size of thermal lesions was investigated. Specifically, thermal lesions volumes generated by 9 focus LTCs with 2 mm or 2.5 mm focus spacing and by a 16 focus LTC with a 2 mm focus spacing were compared. The results indicate that increasing focus spacing or number of foci lead to enlargement of thermal lesion volumes in both the lateral and axial directions. It was demonstrated that a 9 focus LTC with 2mm focus spacing required a total time of 30 min to treat a 2 x 2 x 2 cm<sup>3</sup> tumors, compared to approximately 40 min and 150 min required by

moderately and highly focused spherical transducers respectively.

## **1-Introduction**

It was found that moderately focused spherical transducers offered significantly shorter times for the treatment of a 2 x 2 x 2 cm<sup>3</sup> tissue volume than highly focused spherical transducers. However, there is a limitation on reducing the lesion number because thermal lesions generated by focused spherical transducers are longer in the axial direction than in the lateral direction. Thus, even if the lesion length is identical to the tumors length, the lesion diameter is far from being sufficiently large to cover the tumors in the lateral direction over a few exposures. One approach to enlarge the lesion diameter is to use transducer designs which can generate multiple laterally adjacent foci. When the focus spacing is sufficiently small or the exposure duration is sufficiently long, individual thermal lesions will coalesce into one single large lesion, due to thermal conduction. Three ways to create multi-focus fields are being considered in this chapter. The first way is to use several focused spherical transducers placed adjacent to each other. Each transducer must have a small aperture because the size of available acoustic "windows" at the body surface is limited by bones or air cavities. However, the small aperture reduces the transducer focusing which may lead to damage to tissues surrounding the target. A second way is to use a phased 2-D array [1,2]. A phased 2D array applicator consists of a 2-D grid of small piezoelectric elements, each of which is an individually activated ultrasound source. By activating these elements in a phase delay sequence, interference fields can be created which contain multiple foci. Phased 2-D arrays can also be used to scan and switch between various multiple focus fields electronically. To increase the focusing and to avoid grating lobes [3], a large aperture and small element spacing are required, resulting in a large number of array elements. However, the complexity and cost to build phased array applicators increases dramatically with the number of array elements.

A third way to generate multi-focus fields is to use a combination of a single transducer and a conjugate acoustic lens [4]. Such a lens is formed by cutting the surface of a flat plastics into a 2-D grid of small elements of different thicknesses. The different thicknesses create the phase shifts that are introduced electronically in the case of phased arrays. Whereas elements of a phased array can generate waves with modulated amplitude and phase, elements of a conjugate lens/transducer combination [LTC] produce waves of identical amplitude because the LTC elements are activated by a single ultrasound source. The lack of amplitude modulation may result in some degradation of the focus patterns generated by LTCs. However, the primary advantage of LTCs over phased arrays is that LTCs consisting of a large number of small elements are simple to build and inexpensive. A greater number of elements may allow more complex multi-focus patterns. Although LTCs are less flexible than phased arrays in that an LTC can only produce a single multi-focus pattern, many different lenses may be coupled to a single transducer, and lenses may be designed for individual patients. A theoretical study conducted by Fan and Hyynnen [5] has demonstrated that phased 2-D arrays required significantly shorter treatment times for large tissue volumes than highly focused spherical transducers. The phased 2-D arrays that Fan et al. [2] investigated were spherically focused, to reduce the requirement for small element size. However, the large element size of these arrays, which was  $2 \times 2 \text{ cm}^2$ , limited the range over which foci may be created to the vicinity of the geometric focus of the arrays. The smallest element size being reported for the phased 2-D array design is  $0.65 \times 0.65 \text{ cm}^2$  [1]. This array, which consisted of 256 elements and was geometrically focused to achieve strong focusing, could coagulate tissue volumes of  $0.7\text{cm}(x \text{ axis}) \times 0.7\text{cm}(y \text{ axis}) \times 1.2 \text{ cm}(z \text{ axis})$  using a 9 focus field for a single exposure of 20 S. To date, LTCs have been investigated for mild heating ultrasound treatments by Lalonde and Hunt [4,6]. The element size of  $2 \times 2 \text{ mm}^2$  was chosen for the LTC designs as a compromise between increase in grating lobe levels and surface roughness [7]. Ultrasound scattering from the rough surfaces reduced the efficiency of transmission of ultrasound through the lenses. LTCs of 1000 elements have been constructed, which were able to uniformly heat a  $1 \times 1 \times 1 \text{ cm}^3$  tissue volume to the

hyperthermia temperature by using a 12 focus field [7]. Conjugate lenses can be coupled to either focused or unfocused transducers. It was found that by combining conjugate lenses with focused transducers, the roughness of the lenses was reduced. The intent of this chapter is to evaluate theoretically the ability of LTCs to mimic the focusing of phased arrays and to generate large thermal lesions for high temperature thermal treatments. A design method, based on the pseudoinverse method, was developed to determine the uniform amplitude activation signals for LTCs to produce specified multi-focus fields. The effect of LTCs being restricted to "phase only modulation" on the shape of the thermal lesion volume were examined. The effect of the LTC focus spacing and number of foci on the thermal lesion shape and size was also examined. The time required for a 2 mm spaced, 9 focus LTC to treat a  $2 \times 2 \times 2 \text{ cm}^3$  tumors volume was determined, and compared with those required for the highly and moderately focused spherical transducers.

## 2-Methods

### *LTC Ultrasound Intensity Distribution*

#### *Calculations*

The ultrasound intensity distribution of an LTC was determined using equation (1). This equation was modified from equation 2.1 to take account of the phase delays created by different thicknesses of LTC elements. Note that all LTC elements must share a single particle velocity amplitude value because they are activated by a single source.

$$I(x, y, z) = |P(x, y, z)|^2 = \frac{1}{2c\rho} \left| jK_{wave}c\rho \sum_{n=1}^N \frac{e^{-jK_{wave}d_n}}{2\pi d_n} u_n e^{-j\theta_n} S \right|^2 \quad (1)$$

where

$I$  = intensity at the field point  $(x, y, z)$  [ $\text{W} \cdot \text{cm}^{-2}$ ]

$P$  = complex pressure at the field point  $(x, y, z)$  [ $\text{Pa}$ ].

$U_n$  = amplitude of the complex particle velocity of the lens element  $n$  ( $u_n = u_{n+1}$  [ $\text{cm s}^{-1}$ ]).

$\theta_n$  = phase of the complex particle velocity of the lens element  $n$ .

$N$  = total number of lens elements.

$K_{wave}$  = wave number [ $\text{cm}^{-1}$ ]

$d_n$  = distance [ $\text{cm}$ ] between the lens element  $n$  and the field point  $(x, y, z)$ .

$S$  = surface area of a lens element [ $\text{cm}^2$ ]

$j = \sqrt{-1}$ .

The phase delay ( $-\pi < \theta_n < \pi$ ) was determined from the thickness of the LTC element  $n$  by equation (2).

$$\theta_n = 2\pi f \left( \frac{a_n}{c_{\text{water}}} + \frac{b_n}{c_{\text{lens}}} + \frac{b_n}{c_{\text{water}}} \right) \quad (2)$$

where

$f$  = operating frequency [MHz].

$a_n$  = distance [cm] between the surface of the transducer and the lens.

$b_n$  = thickness [cm] of the lens element  $n$

$c_{\text{water}}$  = speed of sound [ $\text{cm s}^{-1}$ ] in water

$c_{\text{lens}}$  = speed of sound [ $\text{cm s}^{-1}$ ] in the lens

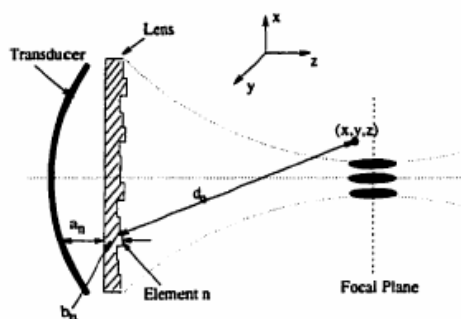


Fig. 3. Coordinates and parameters used in the calculation of LTC field distributions.

### LTC Design Method

An LTC design method, based on the pseudoinverse method [8], was developed here to determine the phase delay ( $\theta_n$ , see equation (1) required for elements of an LTC to produce a specified multi-focus field.

### Pseudoinverse Method

The pseudoinverse method was developed by Ebbini et al. [19] to determine the amplitude and phase ( $u_n$  and  $\theta_n$ , see equation (1) required for phased array elements to produce specified intensity values at intended foci and minimum acoustic power elsewhere (figure (2)). The amplitude values ( $u_n$ ,  $n = 1: N$ ) determined by the pseudoinverse method usually are not identical, whereas in the case of the LTC the amplitude values of all elements must be identical because the lens is coupled to a single transducer. Hence, the pseudoinverse method cannot be directly applied to LTC design. Because only small modifications to the pseudoinverse method was

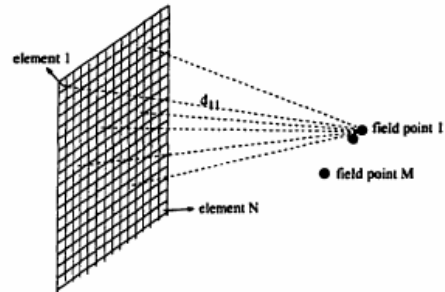


Figure 3.2: Coordinates and parameters used in the pseudoinverse method.

To apply the pseudoinverse method, equation (1) is rewritten in the matrix form:

$$P = HU$$

$$\begin{pmatrix} p_1 e^{-j\phi_1} \\ \vdots \\ p_m e^{-j\phi_m} \\ \vdots \\ p_M e^{-j\phi_M} \end{pmatrix} = j \frac{kcp}{2\pi} S \begin{pmatrix} \frac{e^{jk\omega d_{11}}}{d_{11}} & \dots & \dots & \dots & \dots \\ \dots & \dots & \dots & \dots & \dots \\ \dots & \dots & \frac{e^{jk\omega d_{m1}}}{d_{m1}} & \dots & \dots \\ \dots & \dots & \dots & \ddots & \dots \\ \dots & \dots & \dots & \dots & \frac{e^{jk\omega d_{MN}}}{d_{MN}} \end{pmatrix} \begin{pmatrix} u_1 e^{-j\theta_1} \\ \vdots \\ u_n e^{-j\theta_n} \\ \vdots \\ u_N e^{-j\theta_N} \end{pmatrix} \quad (3)$$

Where

$P$  = vector representing complex field pressure, where  $P_m$  and  $\phi_m$ , represent the amplitude and phase of the complex pressure at the field point  $m$  respectively.

$M$  = number of field points interested.

$H$  =  $M \times N$  matrix describing the propagation of the ultrasound wave from each element of the array to each field point.

$U$  = vector representing complex particle velocity, where  $u_n$  and  $\theta_n$ , represent the amplitude and phase of the complex particle velocity of the phased array element  $n$  respectively.

$N$  = number of phased array elements.

$d_{mn}$  = distance between the field point  $r_n$  and the phased array element  $n$ .

$S$  = surface area of the phased array element.

Equation (3) is solved for  $u$  (If equation (3) had been solved for the design of an LTC, there would be a constraint of  $u_n = u_{n+1}$ . To ensure that solutions to equation (3) exist, the number of field points ( $M$ ) in  $P$  must not be larger than the number of elements ( $N$ ) contained in a phased array. When  $M$  is less than  $N$ , and the positions of these  $M$  field points are such that all of the row vectors of  $H$  are linearly independent, equation (3) possesses an infinite number of solutions [9]. One of these solutions is called the

minimum norm solution (equation (4) [10]), because the norm of this solution ( $\sum_{n=1}^N U_n^2$ ) is the minimum of all solutions.

$$\hat{U}_{\min-norm} = H^* (H H^*)^{-1} \hat{P} \quad (4)$$

Where

$H^*$  = conjugate transpose of  $H$  [9]

Because  $u_n^2$  is proportional to the intensity of the wave generated by the  $n$ th element, the minimum norm solution [MNS] results in a total energy present at the phased array field that is minimized for a given  $P$ . Thus, with the MNS, the likelihood is that the greatest constructive interference, and therefore the greatest pressure amplitude, will occur at the field points specified in  $P$ , the intended foci. However, any solution to equation 3.3. including the MNS, cannot guarantee that the intended foci will be produced. It is possible that field points not specified in  $P$  can possess greater constructive interference than the field points specified in  $P$ . Because the MNS is the most likely solution to produce an intended multi-focus pattern, it was adopted in the design of phased arrays [19,21,23]. Thus,  $M$  can represent the number of foci in the specified field,  $d_m$  is the distance between the focus  $r_m$  and the array element  $n$ , where  $p$ , and  $\#m$  are the relative amplitude and phase of the complex pressure at the focus  $m$ . Because  $H^*(HH^*)^{-1}$  is called the pseudoinverse matrix [66], the use of the MNS (equation (4)) is also called the pseudoinverse method. Since the pseudoinverse method could not be directly applied to the design of LTCs, a method based on the pseudoinverse method was developed for LTC design. The first step in this method was to use the pseudoinverse method to determine the amplitude and phase required for applicator elements to produce specified foci. The second step was to calculate the thicknesses of LTC elements from the phase values determined by the pseudoinverse method using equation 3.2, where the amplitude values determined by the pseudoinverse method was ignored.

### Phase Optimization

The values specified in  $f$  represent the complex pressures at the intended foci. Since the intensity of the wave is a phase-independent quantity, changing the pressure phase value of the acoustic waves at the intended foci will not affect the intensity values at these foci. By varying the relative pressure phase values at the intended foci, it is possible to increase the constructive

interference at these foci, and therefore increase localization of energy in the field. This can be explained mathematically. For each choice of  $P$ , there is an MNS. Given the number, position and pressure amplitudes of foci, there exists one particular phase pattern of foci ( $[\varphi_1, \dots, \varphi_m, \dots, \varphi_M]$ ) which will produce an MNS of the lowest norm. Thus, this phase pattern of foci, compared to other phase patterns of foci, results in the greatest likelihood that the pressure amplitude values at each focus in  $P$  will be greater than that at any other field points. To obtain this particular phase pattern, the following equation was derived [11].

$$G = \frac{\sum_{m=1}^M p_m^2}{\sum_{n=1}^N u_n^2} = \frac{\hat{p}^* p}{\hat{u}_{\min-norm}^* u_{\min-norm}} \quad (5)$$

Where

$G$  = intensity gain, a measure of energy concentration at the foci relative to the entire field.

The phase pattern of  $P$  which minimizes the norm of the MNS  $\sum_{n=1}^N u_n^2$  maximizes  $G$ .

Substituting  $H^*(HH^*)^{-1} P$  (equation (4)) for  $\hat{U}_{\min-norm}$ , equation (5) is expressed as

$$G = \frac{\hat{p}^* \hat{p}}{\hat{p}^* (H H^*)^{-1} \hat{p}} \quad (6)$$

Based on this equation, the phase pattern of  $P$  which maximizes  $G$  can be found iteratively [12-13-14]. A direct solution, according to Ebbini and Cain [11]  $j$  is the phase pattern of the eigenvector that corresponds to the smallest eigenvalue of matrix  $(H H^*)^{-1}$ . Although this solution results in a suboptimal value of  $G$ , it was employed because of its simplicity.

### Summary of LTC Design Procedure

The procedure for the design of an LTC to produce a multi-focus field is summarized as follows:

Step 1: A multi-focus pattern was specified, including the number and position of foci and the pressure amplitudes at these foci. The specified pressure amplitude values were normalized to the maximum of all foci. Parameters of the transducer source were also specified, including the aperture, radius of curvature and operating frequency.

Step 2: Optimization of the phase pattern of the intended foci was performed according to the method discussed in before

Step 3 The MNS was obtained using equation (4).

Step 4: The relative intensity distribution of this LTC was calculated using equation (1) where 0, were equal to the phases of the MNS.

### 3-Results

The LTCs investigated here employed identical spherically focused transducers as the energy source, which had a 10 cm aperture, an 8.5 cm radius of curvature and was operated at a frequency of 1 MHz. This transducer was highly focused so that when multi-focus lenses, which were diverging lenses, were placed in front, sufficiently along focusing could still be maintained in the field. All the LTCs consisted of 2000 elements with each element being  $2 \times 2 \text{ mm}^2$ .

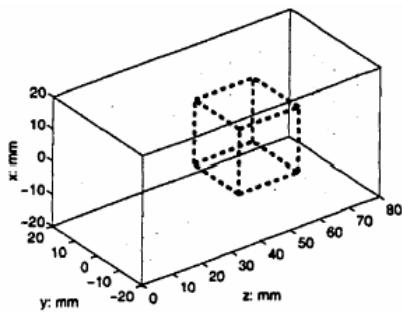


Fig .3. Geometry of the tumor model in Cartesian coordinates. Dashed lines represent the tumor boundary. The body surface is located at the  $z=0 \text{ mm}$  plane.

#### *Comparison of LTCs and phased arrays*

To evaluate if the shape and size of thermal lesions generated by LTCs are similar to those produced by phased array, ultrasound intensity distributions and thermal dose distributions produced by a 2-D phased array and an LTC were compared where these two applicators possessed identical physical parameters, including the diameter, radius of curvature, number of elements and operating frequency, and were designed to produce identical multi-focus patterns. The pseudoinverse method was used in the design of the phased array. The LTC was designed using the method developed in this study. The ultrasound intensity distributions produced by an LTC (denoted as LTC1) and a phased array (denoted as PA) that possessed identical physical parameters and were designed

to produce an identical 9-focus pattern (figure (4) are shown in figure (5). In order to compare the intensity distributions of multi-focus applicators in a useful way, both 2-D contour plots of the applicator focal plane intensity distribution and 6dB and 10dB isosurface plots of the entire applicator field are shown. The 2-D contour plots show that, whereas the intensity values at the foci of PA are identical, intensity values at the foci of LTC1 Vary considerably, but these values were still in a symmetrical pattern. The 6dB isosurface plots indicate considerable difference between the shapes of the focal zone volumes of LTC1 and PA. Whereas the individual focal zones of LTC1 varied in length and diverged at angles at the proximal and distal ends, the individual focal zones of PA were nearly identical in length and all parallel to the applicator axis. The 10dB isosurface plots show the similarity between the focal zone shapes of LTC1 and PA. In both cases, individual focal zones varied in length and diverged at angles at both the proximal and distal ends. Figure (6) plots the lens surface profile of LTC1. The maximum thickness of the elements is 5 mm. The minimum thickness is approximately 0.9 mm. The thermal dose profiles generated by LTC1 and PA for exposure durations of 20 and 50 s are shown in figure (7). The exposures were delivered such that the focal plane of the applicators was at a depth of 5cm below the skin surface. The values for  $I_{sp}$ 's (table(1)) were chosen such that the 60 EM<sub>4</sub> thermal dose contour extended approximately 5 mm beyond the tumor boundary after the exposure. A sufficiently long cooling period (200 and 400 s for exposure durations of 20 and 50 s respectively) was included to allow the tissue to cool to approximately 40°C. This was necessary for calculating the thermal dose to surrounding tissues because a considerable thermal dose was delivered to these tissues after the power was turned off. The thermal lesion volumes (volumes enclosed by the 240EM<sub>43</sub> isosurface) generated by both LTC1 and PA were irregular in shape, with "wings" outside the main lesion volumes. To avoid these "wings" damaging surrounding tissues, sufficiently small  $I_{sp}$ 's were required. However, this also resulted in thermal lesion volumes that were not sufficiently large to cover the tumor volume along the axial direction. Hence, the use of LTC1 and PA to treat a target volume of  $0.8 \text{ cm}(x \text{ axis}) \times 0.8 \text{ cm}(y \text{ axis}) \times 2 \text{ cm}(z \text{ axis})$  for a 20s exposure would lead to 19% and 18% of the target volume being delivered with a thermal dose of less than 240 EM<sub>43</sub>. In the

case of 50s exposure durations, the thermal lesion shapes were less irregular due to the thermal conduction effect. The lateral dimension of the lesion volumes also increased. To treat a larger target volume of  $1 \times 1 \times 2\text{cm}^3$  for a 50s exposure duration, the use of LTCI would lead to a thermal dose of less than  $240\text{EM}_{43}$  delivered to 10% of the target volume, compared to 19% for the use of PA.

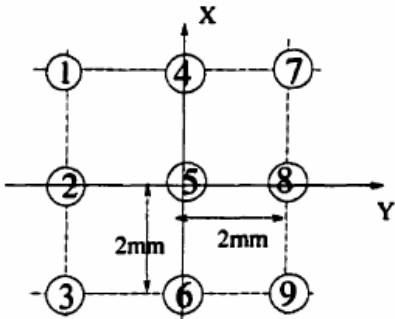


Fig.4. 9 focus pattern with 2 mm focus spacing. All foci were assigned to have the identical pressure amplitude values.

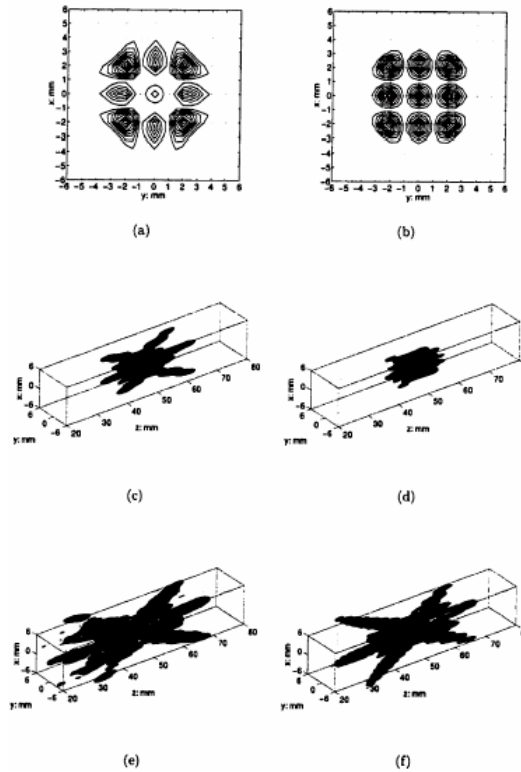


Fig.5. The intensity distributions generated by LTCI (a, c, e), PA (b, d, f). Figures (a) and (b) display the contour plots at the focal plane ( $z=50\text{ mm}$ ), with contours in 10% intervals of the peak value, beginning with the 10% contour. Figures (c) and (d) display the -6dB isosurfaces. Figures (e) and (f) display the -10dB isosurfaces.

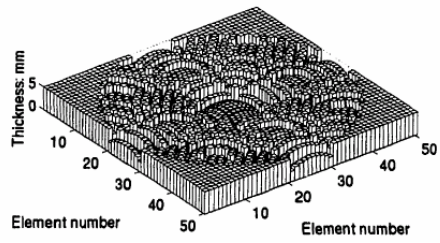


Fig.6. The lens surface profile of LTC1. The element size is  $2 \times 2\text{ mm}^2$ .

	Exposure(s)	$T_{\text{peak}}(\text{C})$	$I_{\text{sp}}(\text{w.cm}^{-2})$
LTC1 (figure7c)	20	66.5	510
LTC1 (figure7e)	50	71.9	270
LTC2 (figure9b)	50	72.4	270
LTC2 (figure9c)	50	65.8	225
LTC3 (figure12b)	50	70.6	270
LTC3 (figure12c)	50	65.6	230
PA(figure7d)	20	80.3	530
PA(figure7f)	50	81	323

Table .1.Values of  $I_{\text{sp}}$  the study.

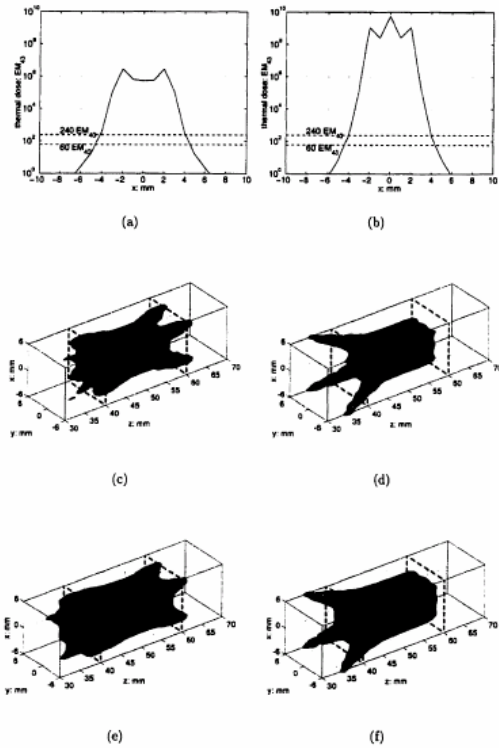


Fig.7. Thermal dose distributions generated by LTC1 (a, c, e) and PA (b, d, f) for 20s (a, b, c, d) and 50s (e, f) exposure durations. Figures (a) and (b) display the thermal dose distributions at  $y=0$  mm and  $z=50$  mm. Figures (b), (c), (d) and (f) display 240 (opaque surface) and 60 Eh& (transparent surface) thermal dose isosurfaces. Dashed lines represent the tumor boundary.

### *Effect of Focus Spacing*

The effect of LTC focus spacing on the shape and size of thermal lesions was examined by comparing the thermal dose profiles generated by two LTCs that produced an identical number of foci, but with different focus spacing. The ultrasound intensity distributions produced by LTC1 and an LTC (denoted as LTCZ) which was designed to produce the same 9 focus pattern (figure (4)) but with a focus spacing of 2.5mm are shown in figure (8). The 2-D contour plots show that the difference between the intensity values at foci was larger in the case of LTC2. The isosurface plots show that the difference between the lengths of individual focal zones was larger in the case of LTCZ. The focal zones of LTCZ also diverged at larger angles than those of LTC1. The thermal dose distributions generated by LTC1 and LTC2 for an exposure durations of 50 s are displayed in figure 9. The exposures were delivered such that

the focal plane of the applicators was at a depth of 5 cm below the skin surface. In the cases of figure (9a) and (9c), the values for  $I_{sp}$ , (table (1)) were chosen such that the 60 EM<sub>43</sub> thermal dose contour extended approximately 5 mm beyond the tumor boundary after the exposure and a cooling period of 400s, which allowed the tissue to cool to approximately 40°C. In the case of figure(9 b), the  $I_{sp}$  value (table 3.1) was chosen to be the same as that used in the case of figures 3.9 (a). Figure (9) shows that, given identical exposure intensities and durations, LTC2 generated a larger thermal lesion volume, in both the axial and lateral directions, than LTC1. If the 60 EM<sub>43</sub> thermal dose contour at 5 mm beyond the tumor boundary was used as the criterion to choose the exposure intensity, the sizes of thermal lesion volumes generated by LTC1 and LTC2 were nearly identical. To treat a  $1 \times 1 \times 2$  cm<sup>3</sup> target volume for an exposure duration of 50s, the use of LTCZ would lead to a thermal dose of less than 240 EMd3 in 7% of the target volume, compared to 10% for the use of LTC 1.

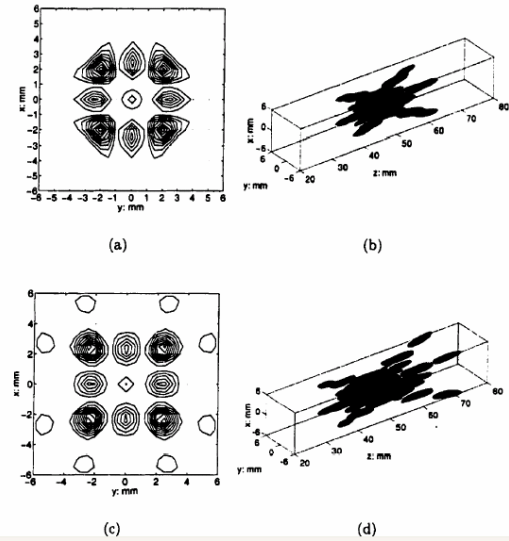


Fig.8. The ultrasound intensity distributions generated by LTC1 (a, b) and LTC2 (c, d). Figures (a) and (c) display the contour plots at the focal plane ( $z=50$  mm), with contours in 10% intervals of the peak value, beginning with the 10% contour. Figures (b) and (d) display the 6dB isosurfaces.

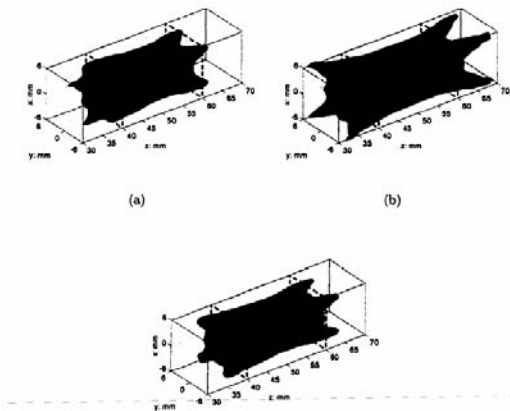


Fig.9. 240 EM<sub>43</sub> (opaque surface) and 60EM<sub>43</sub> (transparent surface) isosurface plots of thermal dose distributions generated by LTC1 (a) and LTC2 (b and c) for a 50s exposure duration. Dashed lines represent the tumor boundary. In the case of figure (b), the I<sub>sp</sub> value was chosen to be the same as that used in the case of figure (a). In the case of figure (c), the values for I<sub>sp</sub> chosen such that the 60 EM<sub>43</sub> thermal dose contour extended approximately 5 mm beyond the tumor boundary after the exposure and a cooling period of 400 s.

#### *Effect of Number of Foci*

The effect of number of foci on the shape and size of thermal lesions was examined by comparing the thermal dose profiles generated by two LTCs with identical focus spacing, but different numbers of foci. The ultrasound intensity distributions produced by LTC1 and an LTC (denoted as LTC3) which was designed to produce the 16 focus pattern (figure 3.10) are illustrated in figure (11). The 2-D contour plots show that the difference between the intensity values at foci was larger in the case of LTC3 than for LTC1. The isosurface plots indicate that the difference between the lengths of individual focal zones was larger in the case of LTC3. The focal zones of LTC3 also diverged at larger angles than those of LTC1.

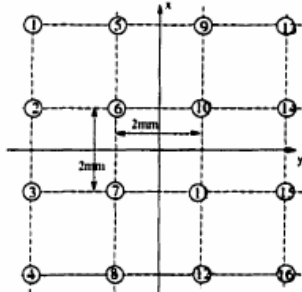


Fig.10. 2mm spaced, 16-focus pattern. All foci were assigned to have the same pressure amplitudes. Foci are numbered as shown.

The thermal dose distributions generated by LTC1 and LTC3 after a 50 exposures duration are displayed in figure (12). The exposures were delivered such that the focal plane of the applicators was at a depth of 5 cm below the skin surface. In the cases of figure (12 -a) and (12-c), the values for I<sub>sp</sub>(table 1) were chosen such that the 60 EM<sub>43</sub> thermal dose contour extended approximately 5 mm beyond the tumor boundary after the exposure and a cooling period of 400 s, which allowed the tissue to cool to approximately 40°C. In the case of figure (12-b), the & value (table1) was chosen to be the same as that used in the case of figures (12- a). Figure (12) shows that , given identical exposure intensities and durations, LTC3 generated a larger thermal lesion volume, in both the axial and lateral directions, than LTC1. If the 60 EM<sub>43</sub> thermal dose contour at 5 mm beyond the tumor boundary was used as the criterion to choose the exposure intensity, the axial dimensions of thermal lesion volumes generated by LTC1 and LTC3 were nearly identical. The lateral dimension of the thermal lesion volume generated by LTC3 was slightly larger than that generated by LTC1. To treat a 1 x 1 x 2cm<sup>3</sup> target volume, the use of LTC3 would lead to a thermal dose less than 240EM<sub>43</sub> in 14% of the target volume, compared to 10% for the use of LTC1.

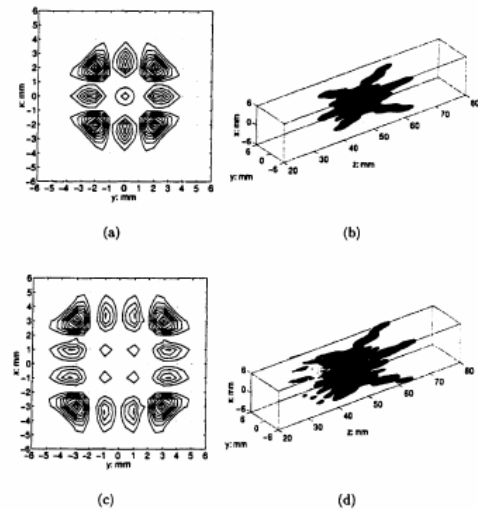


Fig.11. Ultrasound intensity distributions generated by LTC1 (a, b) and LTC3 (c, d). Figures (a) and (c) display the contour plots at the focal plane (z=50mm), with contours in 10% intervals of the peak value, beginning with the 10% contour. Figures (b) and (d) display the 6dB isosurfaces

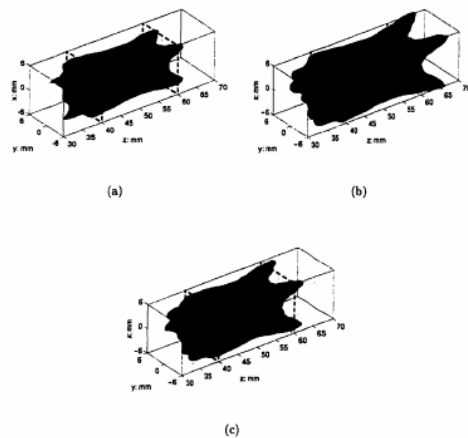


Fig.12. 240 E h 3 (opaque surface) and 60EM<sub>43</sub> (transparent surface) isosurface plots of thermal dose distributions generated by LTC1 (a) and LTC3 (b and c) for a 50s exposure duration. Dashed Lines represent the tumor boundary. In the case of figure (b), the I<sub>sp</sub> value was chosen to be the same as that used in the case of figure (a). In the case of figure (c), the values for I<sub>sp</sub> were chosen such that the 60 EM<sub>43</sub> thermal dose contour extended approximately 5 mm beyond the tumor boundary after the exposure and a cooling period of 400 S.

### *Multiple Exposure treatments of the Tumor*

Since the thermal lesion volumes generated over single exposures by the LTC designs investigated here were not sufficiently large to cover a 2 x 2 x 2 cm<sup>3</sup> tumor volume in the lateral direction, multiple exposures treatments were required. Among all LTC designs investigated here, LTC1 and LTC2 appeared to be preferable because both LTCs can be used to achieve the destruction of 90% of the target volume over a single exposure with the restriction on the thermal dose to the surrounding normal tissue. Thermal lesion volumes generate by LTC2 had more "wings" than those generated by LTC1. The "wings" might overlap when multiple adjacent exposures were delivered to treat large tissue volumes, resulting in damage in surrounding normal tissue regions. Therefore, LTC1 was chosen to be the "optimal" design and the total time required for LTC1 to treat the 2 x 2 x 2 cm<sup>3</sup> tumor volume was determined. Four exposures were required to treat this tissue volume with LTC1 (figure 13). The cooling periods were chosen such that the tissue could cool to approximately 40°C after each exposure. To avoid damage to surrounding tissues due to overlaps between adjacent exposures, the exposure intensities used in the multi-exposure treatment were reduced from 270 W cm<sup>-2</sup> to 250 W cm<sup>-2</sup>. The number of exposures, exposure intensity and duration, cooling period and total

time required for LTC1 to treat the tumor volume are given in table (2). For comparison, the corresponding values for the highly (SPI) and moderately (SP2) . Figures (14) and (15) displays the thermal dose distributions generated by LTC1, SP2 and SPI at the end of the treatment. Due to the gaps between thermal lesion volumes and the irregularity of the thermal lesion shapes, approximately 21% of the tumor volume received a thermal dose of less than 240 EM<sub>43</sub> in the case of LTC1, compared to 26% and 6% for SP2 and SPI respectively. The axial plane thermal dose contour plots indicate that thermal dose gradients generated by LTC1 in the near field are higher than those produced by SP2 and SPI.

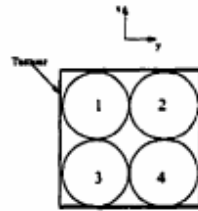


Fig.13. Lateral step pattern for LTC1.

	LTC1	SP2	SP1
Number of exposures	4	25	128
Exposure time (s)	50	10	10
Spatial peak intensity (W.cm <sup>-2</sup> )	250	683	1003
Cooling period (s)	400	90	60
Total time (hour)	.5	.7	2.5
Tumor volume under 240 EM <sub>43</sub>	21%	26%	5%

Table .2. Total treatment times, number of exposures, exposure durations and intensities, cooling times and tumor volume under 240EM<sub>43</sub> for LTC1, SP2 and SPI to treat the tumor volume.

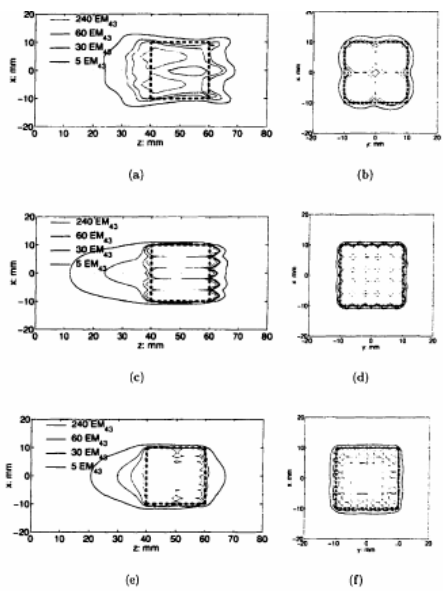


Fig.14. Thermal dose distributions generated by LTCI (a, b), SP2 (c, d) and SPI (e, f) at the end of the treatment. Dashed lines represent the tumor boundary. Figures (a), (c) and (e) display the central axial plane  $y=0\text{mm}$ . Figures (b), (d) and (e) display the lateral plane  $z=50\text{ mm}$ .

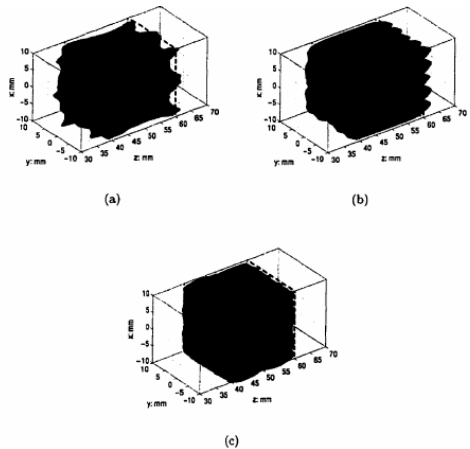


Fig.15. 240 EM<sub>43</sub>(opaque surface) and 60 EM<sub>43</sub> (transparent surface) isosurface plots of thermal dose distributions generated by LTCI (a), SP2 (b) and SPI (c) at the end of the treatment. Dashed lines represent the tumor boundary.

#### 4- Discussion

The results demonstrated that the shape and size of thermal lesion volumes generated by LTCs were similar to those generated by the equivalent phased arrays, which had the same physical parameter as the LTC including the number of elements, aperture, radius of curvature and operating frequency. Hence, the effect of LTCs being restricted to "phase only modulation" had a very small effect on the shape and size of thermal lesion volumes. The LTC design method

was evaluated for designing LTCs to produce symmetrical focus patterns with uniform intensity at foci. It was found that the resulting focus patterns were symmetrical, but with reduced intensity values at the central foci. The effect of this "non-uniform focus intensity" on the thermal lesion shape was small because the tissue located at the central region of the focal zone could be heated through thermal conduction by the foci at the periphery. It can be predicted that the method may not be suitable for designing LTCs to produce the focus fields which contain a large number of foci or large focus spacing. This is because the degradation of intensity values at central foci was already much greater for the 2.5 mm spaced, 9 focus LTC and the 2 mm spaced, 16 focus LTC compared to that for the 2 mm spaced, 9 focus LTC. The results also demonstrated that both the lateral and axial dimension of the thermal lesion volumes increased with LTC focus spacing or number of foci. This finding was expected because an increase in focus spacing or number of foci results in a decrease in applicator focusing, given that the aperture of the applicator remains the same. The decrease in the applicator focusing leads to an enlargement of the focal zone, and therefore the thermal lesion volumes, in both the lateral and axial directions. Increasing the lateral dimension of the thermal lesion volume while keeping the axial dimension unchanged is desirable because it can further decrease the number of lesions required to treat the target volume. A prerequisite for achieving this, by increasing the LTC focus spacing or number of foci, is a corresponding increase in the focusing of the transducer source. Increasing the focusing of an applicator can be achieved by increasing operating frequency, or decreasing the f-number. For treatments of deep-seated tumor volumes, a sufficiently large radius of curvature of the applicator is necessary. Tissue ultrasound attenuation increases linearly with the applicator operating frequency. Therefore, increasing the operating frequency essentially reduces the ability of the applicator to deliver sufficient energy to deep seated tissue volumes. A larger aperture of the applicator is desirable for increasing the focusing. However, in practice, the aperture size is limited by the size of available acoustic "windows" at the body surface. Hence, given a target volume, the minimal number of thermal lesions required for a multi-focus applicator to treat this volume is limited by physical parameters including the depth of the target, the ultrasound attenuation of

the intervening tissues and the size of available acoustic "windows". This minimum lesion number can be achieved by optimizing the treatment parameters such as the physical parameters of the applicator, and exposure duration. The physical parameters of those LTC designs investigated here, including the focus pattern, aperture, radius of curvature and operating frequency, and the exposure durations investigated here were not optimized for the treatment of the target volume. The intent of this study is to demonstrate the potential of LTCs for the treatment of large tissue volumes. The results showed that a 2 mm spaced, 9 focus LTC required a total time of 30 min to treat a 2 x 2 x 2cm<sup>3</sup> tissue volume, 70% and 20% of the time required by the moderately and highly focused spherical transducers respectively. Furthermore, compared to the use of the highly and moderately focused spherical transducers the use of this LTC design resulted in the sharpest thermal dose gradients in the near field region at the end of the treatment, due to the significantly long cooling periods which minimized the heat accumulation in the normal tissue regions. One drawback of the use of LTCs is that long exposure durations of 50s must be adopted to allow the thermal conduction to improve the shape of thermal lesions. When these longer exposure durations, compared to those (10s) used for simple spherically focused transducers, were adopted, the temperature distributions as well as the thermal dose distributions achieved in the tissue would be more dependent on the perfusion. Since perfusion is one of the most uncertain factors in actual treatments, the use of longer exposure durations may lead to difficulties in the control and prediction of thermal lesion formation.

## 5-Conclusions

A theoretical evaluation of the ability of multi-focus acoustic lens/transducer combinations [LTC]to produce large thermal lesion volumes for high temperature focus ultrasound thermal treatments was presented. LTCs were demonstrated to be able to produce thermal lesions with shape and size similar to those generated by phased arrays. Since thermal lesion volumes generated by LTCs were irregular in shape, long exposure durations of 50 s were required for the LTCs to produce thermal lesion volumes of a useful shape. It was also found that, in order to enlarge thermal lesion volume solely along the lateral direction, the LTC focusing needs to be increased. The results demonstrated

that LTCs required significantly shorter treatment times for large tissue volumes than highly and moderately focused spherical transducers.

## 6-Refraances

- [1] D. R. Daum and K. Hynynen. A 256-element ultrasonic phased array system for the treatment of large volumes of deep seated tissue. *IEEE Transactions on Ultrasonic, Ferroelectrics, and Frequency Control*, 46(5) : 1254-1268, 1999.
- [2] X. Fan and K. Hynynen. A study of various parameters of spherically curved phased arrays for noninvasive ultrasound surgery. *Physics in Medicine and Biology*, 41 (4):591-608, April 1996.
- [3] D. H. Turnbull and F. S. Foster. Beam steering with pulsed two dimensional transducer arrays. *IEEE Transactions on Ultrasonic, Ferroelectrics and Frequency Control*, 38:320-333, 1991.
- [4] R. J. Lalonde, A. E. Worthington, and J. W. Hunt. Field conjugate acoustic lenses for ultrasound hyperthermia. *IEEE Transactions on Ultrasonic, Ferroelectrics and Frequency Control*, 29:495-507, 1993.
- [5] X. Fan and K. Hynynen. Ultrasound surgery using multiple sonication treatment time considerations. *Ultrasound in Medicine and Biology*, 22(4) :H1- 82, 1996.
- [6] R. J. Lalonde and J. W. Hunt. Optimizing ultrasound focus distributions for hyperthermia. *IEEE Transactions on Biomedical Engineering*, 42(10) :981-90, 1995.
- [7] R. J. Lalonde. Field conjugate acoustic lenses for ultrasound hyperthermia. PhD thesis, University of Toronto, Ph. D. Thesis, 1994.
- [8] E. S. Ebbini and C. A. Cain. Multiple-focus ultrasound phased array pattern synthesis: optimal driving signal distributions for hyperthermia. *IEEE Transaction on Ultrasonic, Ferroelectrics and Frequency Control*, 36(5):540-548,1989.
- [9] F. K. Storm, W. H. Harrison, and R. S. Elliott. Normal tissue and solid tumor effects of hyperthermia in animal models and clinical trials. *Cancer Research*, 39:2245-2251, 1979.

[10] D. G. Luenberger. Optimization by vector space methods. John Wiley and Sons, Inc., 1969.

[11] E.S. Ebbini and C.A. Cain. Optimization of the intensity gain of multiple focus phased-array heating patterns. International Journal of Hyperthermia, 7:953-973, 1991.

[12] E.S. Ebbini. Deep localized hyperthermia with ultrasound phased arrays using the pseudoinverse pattern synthesis method. PhD dissertation, University of Illinois, urbana, IL, 1990.

[13] P.R. Wheater, H.George,V. G. Daniales ‘Functional histlogy’ medical division of Longman group UK Ltd, 2003.

[14] Tenofsky PL, Beamer L, Smith RS: Ogilvie syndrome as a postoperative complication. Arch Surg; 135(6): 682-6; discussion 686-7, Jun ,2000.